Applied and Environmental Microbiology, Aug. 2011, p. 5604–5609 Vol. 77, No. 16
0099-2240/11/$12.00 doi:10.1128/AEM.02974-10

Role of the Five RNA Helicases in the Adaptive Response of *Bacillus cereus* ATCC 14579 Cells to Temperature, pH, and Oxidative Stresses[▽]

Franck Pandiani,[1,2] Stéphanie Chamot,[1,2] Julien Brillard,[1,2] Frédéric Carlin,[1,2] Christophe Nguyen-the,[1,2] and Véronique Broussolle[1,2]*

INRA, UMR408 Sécurité et Qualité des Produits d'Origine Végétale, F-84000 Avignon, France,[1] and Université d'Avignon et des Pays de Vaucluse, UMR408 Sécurité et Qualité des Produits d'Origine Végétale, F-84000 Avignon, France[2]

Received 20 December 2010/Accepted 14 June 2011

In this study, growth rates and lag times of the five RNA helicase-deleted mutants of *Bacillus cereus* ATCC 14579 were compared to those of the wild-type strain under thermal, oxidative, and pH stresses. Deletion of *cshD* and *cshE* had no impact under any of the tested conditions. Deletion of *cshA*, *cshB*, and *cshC* abolished growth at 12°C, confirming previous results. In addition, we found that each RNA helicase had a role in a specific temperature range: deletion of *cshA* reduced growth at all the tested temperatures up to 45°C, deletion of *cshB* had impact below 30°C and over 37°C, and deletion of *cshC* led mainly to a cold-sensitive phenotype. Under oxidative conditions, deletion of *cshB* and *cshC* reduced growth rate and increased lag time, while deletion of *cshA* increased lag time only with H_2O_2 and reduced growth rate at a high diamide concentration. Growth of the Δ*cshA* strain was affected at a basic pH independently of the temperature, while these conditions had a limited effect on Δ*cshB* and Δ*cshC* strain growth. The RNA helicases CshA, CshB, and CshC could participate in a general adaptation pathway to stressful conditions, with a stronger impact at low temperature and a wider role of CshA.

The DEAD-box RNA helicases are encoded by viral, archaeal, eukaryotic, and prokaryotic genomes (9) and play an important role in RNA processing, transport, and degradation and in many other processes involving RNA (4, 19, 26), such as translation or ribosome biogenesis (10, 11, 22). DEAD-box RNA helicases act as molecular motors that unwind double-stranded RNA, thereby affecting the rearrangement of RNA secondary structures (9, 21). RNA helicases could also be implicated in rearrangement of ribonucleoprotein (RNP) complexes by removing protein from RNA or by the combination of both RNA-unwinding and RNA-annealing activity to promote RNA strand exchange through a potential branch migration (5, 13, 17, 24). Bacterial cells often encounter stressful conditions that tend to decrease the cellular fitness. Consequently, bacteria have to maintain RNA pathway functionalities and control their RNA turnover. Most of the synthesized mRNA is rapidly degraded to allow adaptation to environmental changes (14). RNA helicases could be involved in stress adaptation by maintaining and regulating RNA functions.

Studies reporting the involvement of prokaryotic RNA helicases in the adaptation to abiotic stress mainly deal with response to cold, light, and salt conditions (17). The RNA helicase CrhC maintains the photosynthetic capacity of the cyanobacterium *Synechocystis*. Its expression is regulated by the changes on the redox potential of the electron transport chain caused by variations in light, temperature, and salt concentrations (12). CrhC catalyzes the unwinding of RNA secondary structures but also ensures rearrangements in RNA complexes (5, 25). A *Bacillus subtilis* CshA homolog of *Clostridium perfringens* is involved in the adaptation to oxidative stress, with the corresponding null mutant strain showing better survival under oxidative stress conditions (2). The involvement of RNA helicases in adaptation to environmental stresses has been most often studied in response to low temperature. Thus, *Escherichia coli* RNA helicases CsdA and SrmB allow the correct folding of 50S ribosomal subunits at 20°C (6, 23).

Bacillus cereus is a food-borne pathogen, widely spread in the environment and in a wide range of foods, which consequently has to face many physical and chemical stresses. *B. cereus* RNA helicases have recently been shown to be implicated in cold adaptation (3, 18). Five open reading frames were identified by an *in silico* analysis as encoding the putative RNA helicases CshA to CshE in the *B. cereus* ATCC 14579 genome. Characterization of the five deleted mutants showed that CshA, CshB, and CshC were essential for the adaptation of *B. cereus* at 10°C, while CshD and CshE were not (18).

The aim of this work was to determine whether the Csh RNA helicase family of *B. cereus* could be involved in adaptation to a range of temperatures and oxidative and pH stress conditions that may be encountered by this pathogenic bacterium in the food chain.

MATERIALS AND METHODS

Growth experiments. The *B. cereus* ATCC 14579 strain (wild type [WT]) and the five RNA helicase null mutants (18) were grown in LB broth, pH 6.6, for 16 h at 30°C and 200 rpm. All growth experiments were performed in microplates: each well was inoculated with the appropriate volume of the tested subculture to reach an initial optical density at 600 nm (OD_{600}) of 0.09 in a final volume of 250

* Corresponding author. Mailing address: INRA, UMR408, Site Agroparc, 84914 Avignon Cedex 9, France. Phone: (33) (0) 432 72 25 18. Fax: (33) (0) 432 72 24 92. E-mail: veronique.broussolle@avignon.inra.fr.

▽ Published ahead of print on 24 June 2011.

TABLE 1. Times to detection (Ttds) of *B. cereus* ATCC 14579 and of its RNA helicase isogenic mutants according to growth temperature

Strain	Mean Ttd ± SD (h) at temp[a]:					
	12°C	20°C	30°C	37°C	42°C	45°C
WT	73.8 ± 3.3	3.3 ± 0.6	0.7 ± 0.3	0.8 ± 0.1	0.8 ± 0.0	0.5 ± 0.0
Δ*cshA* mutant	NGO	4.2 ± 0.8*	1.0 ± 0.1*	1.1 ± 0.1*	0.8 ± 0.1	0.8 ± 0.1*
Δ*cshB* mutant	NGO	3.1 ± 0.7	0.8 ± 0.4	ND	0.8 ± 0.1	0.6 ± 0.1*
Δ*cshC* mutant	NGO	5.5 ± 0.8*	1.0 ± 0.1*	ND	0.8 ± 0.0	0.6 ± 0.1*
Δ*cshD* mutant	70.5 ± 6	2.5 ± 0.3*	0.8 ± 0.3	ND	0.7 ± 0.1	0.5 ± 0.0

[a] The Ttd values of the mutant strains were compared to those of the WT. The difference between WT and mutant Ttd values was statistically tested by a paired Student *t* test with 95% confidence, and results were represented as follows: *, significant difference observed between mutant and WT. Ttd values of the Δ*cshE* mutant were not statistically different from that of the WT and were not listed in this table. NGO, no growth observed after 125 h; ND, not done.

μl of LB broth. Microplates were placed in the reading chamber of a Bioscreen C (Oy Growth Curves AB Ltd., Helsinki, Finland), where they were incubated at constant temperature in the range of 10°C to 45°C and continuously shaken at the medium intensity. Bioscreen C was preheated at the set point temperature for 2 h before starting growth experiments, and OD_{600} was recorded every 15 min or every 30 min at low temperature. Hydrogen peroxide and diamide concentrations were adjusted to 4.5 mM and 8.1 mM, respectively, and from 0.5 mM to 1.5 mM by addition of sterile solutions after LB broth sterilization at 120°C for 20 min. To test the effect of pH on *B. cereus* growth, the pH of LB broth was adjusted by the addition of 1 M HCl or 1 M NaOH to 5.0, 7.0, and 8.5 and adjusted again after sterilization with 1 N NaOH if necessary. For each pH and H_2O_2 and diamide concentration, three replicate growth kinetics assays were done with each of at least two independent inocula. CFU were enumerated by plating on LB agar plates 100 μl of serial dilutions of the WT and mutant cells submitted to stress conditions. Plates were then incubated overnight at 37°C.

Catalase activity of WT and mutant cells was tested on LB agar plates, as previously described (8). H_2O_2 concentration was measured during the kinetic assay of incubation of cells with hydrogen peroxide, using the ferrous oxidation in xylenol orange (FOX2) assay, as previously described (20).

Estimation of the growth rate and of the lag time from OD_{600} growth curves. All wells were inoculated at an OD_{600} of at least 0.1. For all conditions, the maximum specific growth rate, μ_{max}, was estimated from the OD_{600} curves as a function of incubation time with the modified Gompertz equation (28)

$$\ln\left(\frac{ABS_t}{ABS_{t0}}\right) = A \cdot \exp\left\{ -\exp\left[\left(\frac{\mu\max \cdot e}{A}\right) \cdot (\lambda - t) + 1\right]\right\} \quad (1)$$

where ABS_t is the OD_{600} of the suspension at the tested time, ABS_{t0} is the initial OD_{600}, A is the logarithmic increase of bacterial population, and λ is the lag time determined by the model. The modified Gompertz equation was described as one of the most appropriately fitting models to determine the specific growth rate (μ_{max}) when the initial OD_{600} of the inoculum is above the Bioscreen C detection threshold (1).

Lag time was estimated by the time to detection (Ttd), corresponding to the abscissa of the point where the initial OD_{600} was increased by 0.05 unit. This point was determined by the equation

$$\text{Ttd} = \left(\frac{((ABS_{t0} + 0.05) - b)}{a}\right) \quad (2)$$

where a represents the slope of the line and b is the y intercept after determining this equation of the curve by a linear regression between the point immediately before and the point immediately after the target OD_{600} + 0.05. WT and mutant strains were paired under each stress condition. The significance of the difference between the WT strain and the mutant strain growth parameters was statistically tested by a bilateral paired Student *t* test with 95% confidence.

Model fit and statistical analysis. Fits were performed by using the least squares criterion. The fitting of the curves was improved by minimizing the sum of the squared residual (SSR) values using the Microsoft Excel solver function between both the growth and the fitted curves where SSR is defined as follows:

$$\text{SSR} = \sum_{i=1}^{n} (\text{value}(i)_{\text{observed}} - \text{value}(i)_{\text{fitted}})^2 \quad (3)$$

Growth parameters μ_{max} and lag of the five *csh*-deleted mutants were determined for each stress condition and were compared to the corresponding WT strain growth parameters in order to determine if the mutants were negatively, positively, or not affected by the tested stress conditions compared to the WT strain.

RESULTS AND DISCUSSION

Responses of *B. cereus* ATCC 14579 RNA helicase mutant strains exposed to temperature, oxidative, and pH stresses were compared to that of the wild type. The two parameters, lag time (Tdt) and growth rate (μ_{max}), were determined to distinguish impact of the RNA helicase on adaptation to the stress conditions upon inoculation and the subsequent growth phase, respectively.

Growth of RNA helicase mutants at different temperatures. Growth of the WT strain occurred at 12°C after a lag time of about 74 h and a maximum growth rate value of about 0.1 h^{-1} (Table 1 and Fig. 1), while no growth was observed for Δ*cshA*, Δ*cshB*, and Δ*cshC* strains at this temperature, even after a 5-day incubation (Table 1). Growth of Δ*cshD* and Δ*cshE* mutants was similar to that of the WT strain at 12°C. At 20°C, the lag time of the WT was shorter than that at 12°C and the μ_{max} reached 0.4 h^{-1}. The Ttd at 20°C of Δ*cshA* and Δ*cshC* strains was longer than that of the WT, while that of the Δ*cshB* strain was not significantly different (Table 1). The longer lag times of

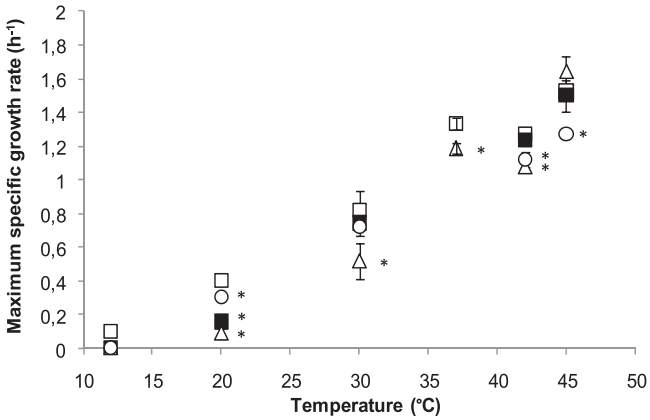

FIG. 1. Effect of temperature on the growth rates of *B. cereus* ATCC 14579 (WT) (□) and Δ*cshA* (△), Δ*cshB* (○), and Δ*cshC* (■) mutant strains growing in LB broth. Values are the means of nine values from three independent cultures; error bars indicate standard deviations, and an asterisk indicates a significant difference ($P < 0.05$) from the μ_{max} of the *B. cereus* WT strain. For clarity, Δ*cshD* and Δ*cshE* strain μ_{max} values were not represented in this figure, as their μ_{max} values were not significantly different from that of the WT strain ($P > 0.05$).

TABLE 2. Times to detection (Ttds) of *B. cereus* ATCC 14579 and of its RNA helicase isogenic mutants according to hydrogen peroxide and diamide concentration at 30°C

Strain	Mean Ttd ± SD (h) at concn of[a]:						
	H_2O_2		Diamide				
	4.5 mM	8.1 mM	0.5 mM	0.8 mM	1 mM	1.3 mM	1.5 mM
WT	4.6 ± 3.0	13.2 ± 1.0	0.8 ± 0.0	1.1 ± 0.1	1.5 ± 0.2	2.9 ± 0.6	3.5 ± 0.6
Δ*cshA* mutant	13.3 ± 3.7*	22.5 ± 3.8*	1.5 ± 0.1*	1.9 ± 0.2*	2.2 ± 0.2*	2.9 ± 0.3	3.2 ± 0.1
Δ*cshB* mutant	9.8 ± 3.7*	NGO	1.0 ± 0.0*	1.5 ± 0.2*	1.6 ± 0.1*	1.7 ± 1.1	3.5 ± 0.6
Δ*cshC* mutant	10.8 ± 2.9*	NGO	1.2 ± 0.1*	1.6 ± 0.1*	2.0 ± 0.1*	3.3 ± 0.3	3.5 ± 0.7

[a] For the statistical procedures and the definition of asterisks, see footnote *a* of Table 1. NGO, no growth observed after 48 h. Ttd values of Δ*cshD* and Δ*cshE* mutants were not statistically different from that of the WT and were not listed in this table.

the Δ*cshA* and Δ*cshC* strains correspond to a phase where cells were adapting to the stress condition and were not due to cell death, as CFU remained relatively constant during the lag phase for both mutant strains (data not shown). The μ_{max} values of Δ*cshA*, Δ*cshC*, and Δ*cshB* strains were 0.1 h^{-1}, 0.2 h^{-1}, and 0.3 h^{-1}, respectively, and were significantly lower than that of the WT (0.4 h^{-1}) (Fig. 1). Δ*cshD* and Δ*cshE* strain Ttd and μ_{max} values were similar to that of the WT (Table 1; Fig. 1; also data not shown). At 30°C, the Δ*cshA* strain was the only mutant with a lower μ_{max} than that of the WT, with a mean value of 0.5 h^{-1}, versus 0.8 h^{-1} for the WT (Fig. 1). Δ*cshA* and Δ*cshC* strains had lag phases of 1.1 h and 1.0 h, respectively, indicating that these mutant strains needed 0.4 h more than the WT did to adapt and start to grow at this temperature (Table 1). When strains were grown at 37°C, the Δ*cshA* mutant Ttd (1.1 h) and maximum growth rate (1.2 h^{-1}) were still slightly lower than those of the WT (Fig. 1 and Table 1). We also tested the growth capacity of the *csh* mutants beyond the optimal temperature, at 42°C and 45°C: at 42°C, the Ttds of the five *csh* mutants were similar to that of the WT (Table 1) but the μ_{max} values of the Δ*cshA* and Δ*cshB* strains, both equal to 1.1 h^{-1}, were lower than the 1.3-h^{-1} value observed for the WT (Fig. 1). All mutants grew similarly to the WT at 45°C, except the Δ*cshB* strain, which had a significantly lower μ_{max} (1.3 h^{-1}) than did the WT (1.5 h^{-1}). Compared to the WT, the Ttds of Δ*cshA*, Δ*cshB*, and Δ*cshC* strains were 10 to 50% longer (Table 1).

The RNA helicases CshA, CshB, and CshC were all required for *B. cereus* growth at low temperatures but not over the same range of temperatures, indicating that they probably do not act all by the same mechanism. Indeed, previous experiments of cross complementation of Δ*cshB* and Δ*cshC* strains with a *cshA* copy in *trans* showed that the overexpression of *cshA* was able to restore the WT phenotype in the Δ*cshB* mutant but not in the Δ*cshC* mutant at low temperature (18). These experiments suggest that CshA and CshB could have overlapping functions and are consistent with a similar thermal requirement for CshA and CshB. CshC may have functionalities complementary to those of CshA. It is the only RNA helicase acting specifically during cold acclimation and may act differently. Because of its strong involvement at low temperature and its role at all other tested temperatures, CshA may have both a major role in cold stress and an important role as an essential protein for *B. cereus* growth. The RNA helicase requirement for *B. cereus* growth at different temperatures contrasted with *B. subtilis*, as the deletion of the *cshA* or *cshB* gene did not reduce the growth rate of these bacteria at 15°C (10). In *E. coli*, the deletion of the genes encoding CsdA or SrmB RNA helicases led to a cold-sensitive phenotype at 20°C (6, 7). Some RNA helicases of *B. cereus* are required both for adaptation, as revealed by an increase of lag time in the mutant, and for maintaining an optimal growth rate under stressful conditions, as revealed by a lower μ_{max} in the mutant.

Growth of *csh* mutants exposed to H_2O_2 and diamide. Growth of the WT and the five *csh* mutant strains was tested at 30°C with 4.5 mM and 8.1 mM hydrogen peroxide. The Ttd of the WT increased from 0.7 h (control) to 4.6 h with 4.5 mM H_2O_2 and to 13.2 h with 8.5 mM H_2O_2 (Table 1 and Table 2), while there was no significant difference in μ_{max} values at the tested H_2O_2 concentrations (Fig. 2).

In the presence of 4.5 mM H_2O_2, the Ttds of Δ*cshA*, Δ*cshB*, and Δ*cshC* strains, equal to 13.3 h, 9.8 h, and 10.8 h, respectively, were at least 2-fold higher than the lag time of the WT (Table 2). The μ_{max} of Δ*cshA* (0.3 h^{-1}) was lower than that of the WT (0.7 h^{-1}), while the μ_{max} values of Δ*cshB* and Δ*cshC* strains were similar to that of the WT. We observed a 2-log decrease in Δ*cshB* and Δ*cshC* populations and a 5-log decrease for Δ*cshA* cells during the lag time (data not shown). This clearly shows that the growth of the Δ*cshA* strain, observed

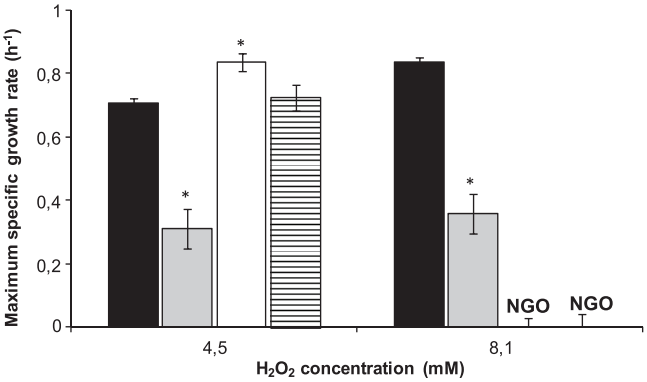

FIG. 2. Effect of H_2O_2 concentration on the growth rate of *B. cereus* ATCC 14579 (black bars) and Δ*cshA* (gray bars), Δ*cshB* (white bar), and Δ*cshC* (striped bar) mutants in LB broth at 30°C. Values are the means of six values from two independent cultures, error bars indicate standard deviations, and an asterisk indicates a significant variation of the μ_{max} value from that of WT. Δ*cshD* and Δ*cshE* strain μ_{max} values were never statistically different ($P > 0.05$) from that of the WT and were not represented. NGO, no growth observed after 48 h for Δ*cshB* and Δ*cshC* strains.

TABLE 3. Times to detection (Ttds) of *B. cereus* ATCC 14579 WT and Δ*cshA* mutant according to diamide concentration at 37°C

Strain	Mean Ttd ± SD (h) at concn of[a]:						
	H_2O_2		Diamide				
	4.5 mM	8.1 mM	0.5 mM	0.8 mM	1 mM	1.3 mM	1.5 mM
WT	9.2 ± 0.3	ND	0.9 ± 0.2	1.6 ± 0.4	2.7 ± 0.2	4.4 ± 0.6	5.9 ± 0.3
Δ*cshA* mutant	10.2 ± 0.7*	ND	1.2 ± 0.4	2.1 ± 0.5*	2.7 ± 0.4	4.6 ± 1.2	4.4 ± 2.6

[a] For statistical procedures and definitions of abbreviations and asterisks, see footnote *a* of Table 1.

after a long lag phase in the presence of 4.5 mM H_2O_2, was due to a very low number of surviving cells. This suggests that CshA may have a role in resistance of *B. cereus* to hydrogen peroxide stress. It was previously reported that a *C. perfringens* RNA helicase was involved in the oxidative response, but its exact role was not described (2).

B. cereus possesses a catalase activity, which was also present in the mutant cells (data not shown). We determined that the 4.5 mM H_2O_2 concentration was rapidly reduced to 50 nM in the presence of *B. cereus* WT or mutant cells but remained constant after extended incubation. We checked, as a control, that H_2O_2 was not degraded during incubation at 30°C in the absence of *B. cereus* cells. *B. cereus* cells were consequently rapidly exposed to a lower concentration of H_2O_2 than initially planned, but the lag phase was clearly due to this residual H_2O_2 concentration.

When the concentration of H_2O_2 was increased to 8.1 mM, the WT strain needed 13.2 h to start its growth and the Ttd of the Δ*cshA* strain (22.5 h) was markedly longer than the WT Ttd. No growth of Δ*cshB* and Δ*cshC* strains was detected with 8.1 mM H_2O_2 (Table 2). Growth of the Δ*cshA* strain was impaired with a lower μ_{max} (0.3 h^{-1}) than that of the WT (0.7 h^{-1}) (Fig. 2). The μ_{max} values and the Ttds of Δ*cshD* and Δ*cshE* strains were not different from those of the WT for the two concentrations of H_2O_2 at 30°C (data not shown). We showed that Δ*cshA* growth was less affected at 37°C than at 30°C, so we tested the effect of H_2O_2 at 37°C: the Δ*cshA* strain had a significantly higher Ttd than did the WT in the presence of 4.5 mM H_2O_2 (Table 3).

The effect of diamide at concentrations ranging between 0.5 mM and 1.5 mM was tested on WT and mutant strains at 30°C: the increasing concentrations of diamide increased the lag time for WT but had no significant impact on the maximum specific growth rate (Table 2 and Fig. 3A). The Ttds of Δ*cshA*, Δ*cshB*, and Δ*cshC* strains were significantly higher than that of the WT for 0.5, 0.8, and 1.0 mM diamide but not for higher concentrations (Table 2), while Δ*cshD* and Δ*cshE* strain Ttd values were not modified at all (not shown). Whatever the concentration of diamide, Δ*cshA*, Δ*cshB*, and Δ*cshC* strains had a significantly lower μ_{max} than did the WT (Fig. 3A) while Δ*cshD* and Δ*cshE* strains grew similarly to the WT. When tested at 37°C, the Ttd of the Δ*cshA* strain was similar to that of the WT, except at the 0.8 mM concentration (Table 3). The growth rate of the Δ*cshA* strain was similar to that of the WT for 0.5 mM, 0.8 mM, and 1.0 mM diamide but was significantly lower at 1.3 and 1.5 mM diamide (Fig. 3B).

RNA helicases act as chaperones to restore functionalities of RNA molecules altered by oxidative agents. However, CshA, CshB, and CshC do not seem to have the same impact during growth with oxidative agents. Hydrogen peroxide is an oxygen-reactive molecule that could damage biological targets by rupture of molecular bonds and then modification of their conformations and functions. The role of RNA helicases in resistance or adaptation to H_2O_2 stress had not

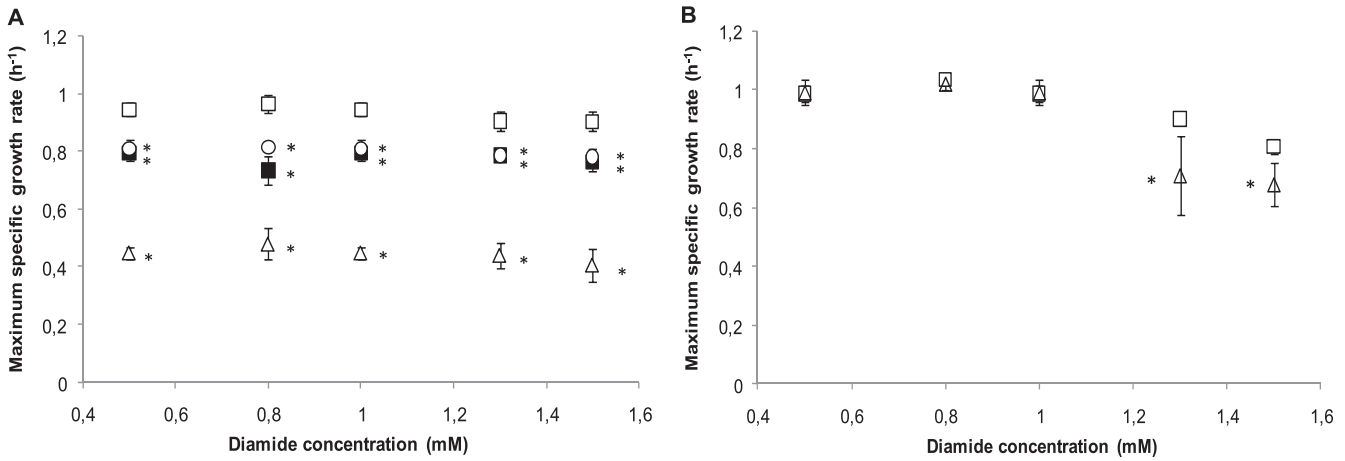

FIG. 3. Effect of diamide concentration at 30°C on the μ_{max} values of *B. cereus* ATCC 14579 (WT) (□) and Δ*cshA* (△), Δ*cshB* (○), and Δ*cshC* (■) mutant strains in LB broth (A) and at 37°C on the μ_{max} values of WT strain (□) and of the Δ*cshA* mutant (△) (B). Values are the means of six values from two independent cultures, error bars indicate standard deviations, and an asterisk indicates a significant variation of the μ_{max} value from that of WT. μ_{max} values of Δ*cshD* and Δ*cshE* strains were never statistically different from the WT μ_{max} and were not represented.

TABLE 4. Times to detection (Ttds) of *B. cereus* ATCC 14579 and of its RNA helicase isogenic mutants according to pH values at 30°C

Strain	Mean Ttd ± SD (h) at pH[a]:		
	5.0	7.0	8.5
WT	2.6 ± 0.4	0.7 ± 0.3	1.0 ± 0.1
Δ*cshA* mutant	4.1 ± 0.4*	0.9 ± 0.4	1.2 ± 0.1
Δ*cshB* mutant	2.2 ± 0.3	0.8 ± 0.4	1.0 ± 0.1
Δ*cshC* mutant	3.8 ± 0.5*	0.8 ± 0.3	1.3 ± 0.1

[a] For statistical procedures and definition of asterisks, see footnote *a* of Table 1. Ttd values of Δ*cshD* and Δ*cshE* mutants were not statistically different from that of the WT and were not listed in this table.

TABLE 5. Times to detection (Ttds) of *B. cereus* ATCC 14579 WT and Δ*cshA* mutant according to pH values at 37°C

Strain	Mean Ttd ± SD (h) at pH[a]:		
	5.0	7.0	8.5
WT	1.7 ± 0.2	1.1 ± 0.1	0.4 ± 0.1
Δ*cshA* mutant	2.6 ± 0.3*	0.9 ± 0.1*	0.7 ± 0.1*

[a] For statistical procedures and definition of asterisks, see footnote *a* of Table 1.

been investigated so far. H_2O_2 can cause the dissociation of ribosomes in 30S and 50S subunits (16). Modification of ribosome properties or ribosome folding could explain why RNA helicases seem to be essential for the adaptation to hydrogen peroxide. The lesser role of RNA helicase in the presence of diamide than in the presence of H_2O_2 could be due to different modes of action of these oxidative compounds.

CshA, CshB, and CshC are required for optimal growth in both oxidative and low-temperature environments. Oxidative compounds could also prevent the action of enzymes which are involved in the adaptive modification of membrane fatty acid profiles. These modifications are required during cold adaptation, and that could partially explain the connection between these two stresses (27).

Growth of *csh* mutants at acid and basic pHs. Growth of WT and the five *csh* mutant strains was studied at 30°C and at pH 5.0, pH 7.0, and pH 8.5. The Ttd of the WT at pH 5.0 was longer than that at pH 7.0, indicating a stress condition for *B. cereus*, as already described elsewhere (15). The Ttds of Δ*cshA* and Δ*cshC* strains, 4.1 h and 3.8 h, respectively, were twice as long as that for the WT (Table 4). The longer lag phases of the mutant strains were not due to cell death, as determined by CFU counts (data not shown). At pH 5.0, all the mutants had a maximum specific growth rate similar to that of the WT (Fig. 4A).

WT strain growth rates at pH 8.5 and pH 7.0 were similar, indicating that such basic pH was not a stress condition for *B. cereus*. The Ttds of the five mutant strains were similar to that of the WT at pH 8.5 (Table 4), but the μ_{max} values of all mutants, except the Δ*cshD* and Δ*cshE* strains, were lower (Fig. 4A). At 37°C, the lag time of the Δ*cshA* strain was higher than that of the WT at both pH 5.0 and pH 8.0 (Table 5). At pH 8.0 and 37°C, the Δ*cshA* mutant μ_{max} was significantly lower than the WT μ_{max}, but the difference was reduced compared to that at 30°C (Fig. 4B). Lag times and μ_{max} values of Δ*cshD* and Δ*cshE* mutants at pH 5.0, 7.0, and 8.5 were not different from those of WT at 30°C (data not shown).

CshA is involved in basic pH adaptation, the absence of CshB impacted on the μ_{max} value at basic pH but not on adaptation, and CshC was required during adaptation to acid conditions and also for maintaining an optimal growth rate under basic growth conditions. Basic conditions could modify mRNA and rRNA conformations, leading to a loss of functionality and consequently requiring the action of RNA helicases as chaperones (17).

In conclusion, the RNA helicases CshA, CshB, and CshC participate in adaptation to several stressful conditions, each RNA helicase with some specificity, CshA having presumably the widest role. These three RNA helicases had the strongest impact, with a total absence of growth of the deletion mutants

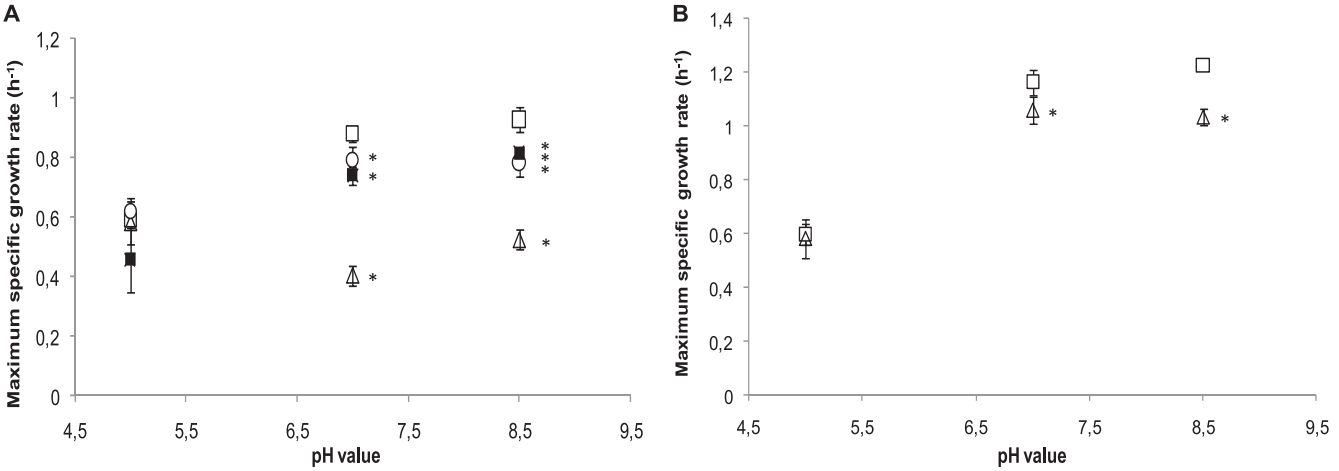

FIG. 4. Effect of pH on μ_{max} at 30°C of *B. cereus* ATCC 14579 (WT) (□) and Δ*cshA* (△), Δ*cshB* (○), and Δ*cshC* (■) mutant strains in LB broth (A) and on μ_{max} at 37°C of the WT strain (□) and the Δ*cshA* mutant (△) (B). Values are the means of six values from two independent cultures, error bars indicate standard deviations, and an asterisk indicates a significant variation of the μ_{max} value from that of WT ($P < 0.05$). For clarity, Δ*cshD* and Δ*cshE* strain μ_{max} values were not represented, as they were not statistically different from the WT μ_{max} ($P > 0.05$).

at low temperature and growth highly affected in the presence of H_2O_2. In contrast, CshD and CshE are not involved in adaptation to the abiotic stress tested in this work, and the function of these two RNA helicases in *B. cereus* is still unknown.

ACKNOWLEDGMENTS

We thank Isabelle Iost and A. J. Carpousis for very helpful discussions and Marie-José Vallier and Isabelle-Orlane Patrascu for technical assistance.

The financial support for F.P. is from the INRA and the Regional Council Provence Alpes Côte d'Azur. This work was supported by the Agence Nationale de la Recherche (ANR) (France) under the ANR-05-PNRA-013 *B. cereus* contract.

REFERENCES

1. **Augustin, J. C., L. Rosso, and V. Carlier.** 1999. Estimation of temperature dependent growth rate and lag time of *Listeria monocytogenes* by optical density measurements. J. Microbiol. Methods **38:**137–146.
2. **Briolat, V., and G. Reysset.** 2002. Identification of the *Clostridium perfringens* genes involved in the adaptive response to oxidative stress. J. Bacteriol. **184:**2333–2343.
3. **Broussolle, V., et al.** 2010. Insertional mutagenesis reveals genes involved in *Bacillus cereus* ATCC 14579 growth at low temperature. FEMS Microbiol. Lett. **306:**177–183.
4. **Carpousis, A. J.** 2007. The RNA degradosome of *Escherichia coli*: an mRNA-degrading machine assembled on RNase E. Annu. Rev. Microbiol. **61:**71–87.
5. **Chamot, D., K. R. Colvin, S. L. Kujat-Choy, and G. W. Owttrim.** 2005. RNA structural rearrangement via unwinding and annealing by the cyanobacterial RNA helicase, CrhR. J. Biol. Chem. **280:**2036–2044.
6. **Charollais, J., M. Dreyfus, and I. Iost.** 2004. CsdA, a cold-shock RNA helicase from *Escherichia coli*, is involved in the biogenesis of 50S ribosomal subunit. Nucleic Acids Res. **32:**2751–2759.
7. **Charollais, J., D. Pflieger, J. Vinh, M. Dreyfus, and I. Iost.** 2003. The DEAD-box RNA helicase SrmB is involved in the assembly of 50S ribosomal subunits in *Escherichia coli*. Mol. Microbiol. **48:**1253–1265.
8. **Claus, D., and R. C. W. Berkeley.** 1986. Genus *Bacillus* Cohn 1872, 174^{AL}, p. 1105–1139. *In* P. H. A. Sneath, N. S. Mair, M. E. Sharpe, and J. G. Holt (ed.), Bergey's manual of systematic bacteriology, vol. 2. Williams & Wilkins, Baltimore, MD.
9. **Cordin, O., J. Banroques, N. K. Tanner, and P. Linder.** 2006. The DEAD-box protein family of RNA helicases. Gene **367:**17–37.
10. **Hunger, K., C. L. Beckering, F. Wiegeshoff, P. L. Graumann, and M. A. Marahiel.** 2006. Cold-induced putative DEAD box RNA helicases CshA and CshB are essential for cold adaptation and interact with cold shock protein B in *Bacillus subtilis*. J. Bacteriol. **188:**240–248.
11. **Jones, P. G., M. Mitta, Y. Kim, W. N. Jiang, and M. Inouye.** 1996. Cold shock induces a major ribosomal-associated protein that unwinds double-stranded RNA in *Escherichia coli*. Proc. Natl. Acad. Sci. U. S. A. **93:**76–80.
12. **Kujat, S. L., and G. W. Owttrim.** 2000. Redox-regulated RNA helicase expression. Plant Physiol. **124:**703–713.
13. **Linder, P.** 2006. Dead-box proteins: a family affair—active and passive players in RNP-remodeling. Nucleic Acids Res. **34:**4168–4180.
14. **Marcaida, M. J., M. A. DePristo, V. Chandran, A. J. Carpousis, and B. F. Luisi.** 2006. The RNA degradosome: life in the fast lane of adaptive molecular evolution. Trends Biochem. Sci. **31:**359–365.
15. **Mols, M., R. van Kranenburg, C. C. J. van Melis, R. Moezelaar, and T. Abee.** 2010. Analysis of acid-stressed *Bacillus cereus* reveals a major oxidative response and inactivation-associated radical formation. Environ. Microbiol. **12:**873–885.
16. **Nakamura, K., and T. Tamaoki.** 1968. Reversible dissociation of *Escherichia coli* ribosomes by hydrogen peroxide. Biochim. Biophys. Acta **161:**368–376.
17. **Owttrim, G. W.** 2006. RNA helicases and abiotic stress. Nucleic Acids Res. **34:**3220–3230.
18. **Pandiani, F., et al.** 2010. Differential involvement of the five RNA helicases in adaptation of *Bacillus cereus* ATCC 14579 to low growth temperature. Appl. Environ. Microbiol. **76:**6692–6697.
19. **Regonesi, M. E., et al.** 2006. Analysis of the *Escherichia coli* RNA degradosome composition by a proteomic approach. Biochimie **88:**151–161.
20. **Sodergren, E., J. Nourooz-Zadeh, L. Berglund, and B. Vessby.** 1998. Re-evaluation of the ferrous oxidation in xylenol orange assay for the measurement of plasma lipid hydroperoxides. J. Biochem. Biophys. Methods **37:**137–146.
21. **Story, R. M., H. Li, and J. N. Abelson.** 2001. Crystal structure of a DEAD box protein from the hyperthermophile *Methanococcus jannaschii*. Proc. Natl. Acad. Sci. U. S. A. **98:**1465–1470.
22. **Tanner, N. K., and P. Linder.** 2001. DExD/H box RNA helicases: from generic motors to specific dissociation functions. Mol. Cell **8:**251–262.
23. **Trubetskoy, D., F. Proux, F. Allemand, M. Dreyfus, and I. Iost.** 2009. SrmB, a DEAD-box helicase involved in *Escherichia coli* ribosome assembly, is specifically targeted to 23S rRNA in vivo. Nucleic Acids Res. **37:**6540–6549.
24. **Valdez, B. C., D. Henning, K. Perumal, and H. Busch.** 1997. RNA-unwinding and RNA-folding activities of RNA helicase II Gu—two activities in separate domains of the same protein. Eur. J. Biochem. **250:**800–807.
25. **Vinnemeier, J., and M. Hagemann.** 1999. Identification of salt-regulated genes in the genome of the cyanobacterium *Synechocystis* sp strain PCC 6803 by subtractive RNA hybridization. Arch. Microbiol. **172:**377–386.
26. **Worrall, J. A. R., et al.** 2008. Reconstitution and analysis of the multienzyme *Escherichia coli* RNA degradosome. J. Mol. Biol. **382:**870–883.
27. **Zuber, P.** 2009. Management of oxidative stress in *Bacillus*. Annu. Rev. Microbiol. **63:**575–597.
28. **Zwietering, M. H., I. Jongenburger, F. M. Rombouts, and K. Vantriet.** 1990. Modelling of the bacterial growth curve. Appl. Environ. Microbiol. **56:**1875–1881.